SPIN POLARIZATION SIMULATIONS FOR THE FUTURE CIRCULAR COLLIDER e+e- USING BMAD[*]

Y. Wu[1,†], F. Carlier[2], L. Van Riesen-Haupt[1], T. Pieloni[1]

[1]École Polytechnique Fédérale de Lausanne (EPFL), Lausanne, Switzerland

[2]European Organization for Nuclear Research (CERN), Geneva, Switzerland

Abstract

Measurements of particle properties with unprecedented accuracy in the Future Circular Collider e+e- (FCC-ee) are reliant on the high precision center-of-mass energy calibration, which could be realized via resonant depolarization measurements. The obtainable equilibrium spin polarization levels under the influence of lattice imperfections should be estimated via spin polarization simulations. An early-stage exploration of spin simulations in the FCC-ee has been conducted using Bmad. An effective model has been used to generate residual errors for the simulation of realistic orbits after lattice corrections. The influences of depolarization effects near the first-order spin-orbit resonances are displayed in linear polarization simulations, highlighting the demand for good closed orbit control. Furthermore, the first attempts at performing nonlinear spin tracking simulations in the FCC-ee reveals the full impact of lattice perturbations.

INTRODUCTION

The Future Circular Collider (FCC) was proposed to push both the energy and intensity frontiers of particle physics [1]. The FCC-ee, which is an electron-positron collider, as the first step of the FCC project, is designed to operate on multiple center-of-mass collision energies $\sqrt{s}$ between 88 GeV and 365 GeV for the production of Z^0 bosons ($\sqrt{s} \sim 91$ GeV), WW pairs ($\sqrt{s} \sim 160$ GeV), Higgs bosons ($\sqrt{s} \sim 240$ GeV) and top quark pairs ($\sqrt{s} \sim 350 - 365$ GeV) [1, 2].

The current precision requirements at Z mass and W mass are 4 keV and 250 keV respectively [3]. Resonant depolarization is a high precision energy calibration method that has been used in previous lepton machines such as the Large Electron–Positron Collider (LEP) [4], and is the proposed method in the FCC-ee to reach the unprecedented precision target at the Z and W pair threshold [2]. Spin polarization simulations are required to validate this energy calibration method in the FCC-ee by investigating the effects of lattice perturbations on spins. A minimum of 10% transverse polarization level at equilibrium should be guaranteed under various possible lattice conditions in order to ensure accurate energy calibration measurements [5].

Basics of Spin Dynamics

The spin precession motion in electromagnetic fields can be described by the Thomas-Bargmann-Michel-Telegdi (T-BMT) equation [6, 7],

$$\frac{d\vec{S}}{dt} = \vec{\Omega}_{\mathrm{BMT}} \times \vec{S}, \qquad (1)$$

where $\vec{S}$ is the spin expectation and the precession vector $\vec{\Omega}_{\mathrm{BMT}}$ is in the form of [8]

$$\vec{\Omega}_{\mathrm{BMT}} = -\frac{e}{m}\left[\left(a + \frac{1}{\gamma}\right)\vec{B} - \frac{a\gamma}{\gamma + 1}\vec{\beta}(\vec{\beta} \cdot \vec{B}) - \left(a + \frac{1}{\gamma + 1}\right)\vec{\beta} \times \vec{E}\right], \qquad (2)$$

where e and m are the particle charge and mass respectively, $\vec{\beta}$ and γ are the relativistic factors, $\vec{B}$ and $\vec{E}$ are the magnetic and electric fields, and the gyromagnetic anomaly a is approximately 0.0011597 for electrons and positrons. The precession vector can be decomposed into the periodic closed orbit term $\vec{\Omega}^{c.o}(s)$ and the other term brought by synchrobetatron motions $\vec{\omega}^{s.b}(\vec{u}; s)$

$$\vec{\Omega}_{\mathrm{BMT}}(\vec{u}; s) = \vec{\Omega}^{c.o}(s) + \vec{\omega}^{s.b}(\vec{u}; s), \qquad (3)$$

where s is the azimuthal position and vector $\vec{u} \equiv (x, x', y, y', z, \delta)$ denotes the phase space position of a particle with δ being the relative energy deviation $\delta = \Delta E/E_0$ [8]. The unit length one-turn periodic solution of the T-BMT equation on the closed orbit is denoted as $\hat{n}_0$, which is the stable spin direction on the closed orbit [9, 10]. In a perfectly aligned flat machine, arbitrary spins on the closed orbit will perform $a\gamma$ precessions around $\hat{n}_0$ during one orbital revolution, which is the closed orbit spin tune ν_0. Nevertheless, ν_0 will experience a slight deviation from $a\gamma$ when there are errors and misalignments in the machine [10].

The emission of synchrotron radiation when electrons and positrons are moving in the ring can enable spin flip which switches the spin direction between spin up and down, through the Sokolov-Ternov effect [11]. The slight difference in the transition rates between two spin states allows an accumulation of polarization along the opposite direction of the magnetic field for electrons. An equilibrium polarization level of $P_{ST} \simeq 92.38\%$ can be reached in uniform magnetic fields, while in arbitrary fields it can be estimated with the following equation [12, 13]

$$\vec{P}_{bks} = -\frac{8}{5\sqrt{3}}\hat{n}_0 \frac{\oint ds \frac{\hat{n}_0(s) \cdot \hat{b}(s)}{|\rho(s)|^3}}{\oint ds \frac{[1 - \frac{2}{9}(\hat{n}_0 \cdot \hat{s})^2]}{|\rho(s)|^3}}, \qquad (4)$$

where ρ represents the instantaneous bending radius, $\hat{b} = (\hat{s} \times \dot{\hat{s}})/|\dot{\hat{s}}|$ is the magnetic field direction, and $\hat{s}$ is the unit

vector of motion direction. The polarization is accumulated at a rate of

$$\tau_{bks}^{-1} = \frac{5\sqrt{3}}{8} \frac{r_e \gamma^5 \hbar}{m_e} \frac{1}{C} \oint \mathrm{d}s \frac{\left[1 - \frac{2}{9}(\hat{n}_0 \cdot \hat{s})^2\right]}{|\rho(s)|^3}, \qquad (5)$$

where m_e is the electron mass and C is the machine circumference.

The spin diffusion caused by stochastic photon emissions during synchrotron radiation results in radiative depolarization, which competes with polarization accumulation, bringing an equilibrium polarization level that can be estimated via the Derbenev–Kondratenko–Mane (DKM) formula [14, 15],

$$P_{dk} = -\frac{8}{5\sqrt{3}} \times \frac{\oint \mathrm{d}s \left\langle \frac{1}{|\rho(s)|^3} \hat{b} \cdot \left(\hat{n} - \frac{\partial \hat{n}}{\partial \delta}\right)\right\rangle_s}{\oint \mathrm{d}s \left\langle \frac{1}{|\rho(s)|^3} \left(1 - \frac{2}{9}(\hat{n} \cdot \hat{s})^2 + \frac{11}{18}\left(\frac{\partial \hat{n}}{\partial \delta}\right)^2\right)\right\rangle_s}, \qquad (6)$$

where $\hat{n}(\vec{u}; s)$ is the equilibrium polarization direction at each phase space and azimuthal position, and $\langle\rangle_s$ denotes the average over phase space at position s. Radiative depolarization is quantified by the spin-orbit coupling function $\partial\hat{n}/\partial\delta$, with the depolarization rate being

$$\tau_{dep}^{-1} = \frac{5\sqrt{3}}{8} \frac{r_e \gamma^5 \hbar}{m_e} \frac{1}{C} \oint \mathrm{d}s \left\langle \frac{\frac{11}{18}(\frac{\partial\hat{n}}{\partial\delta})^2}{|\rho(s)|^3}\right\rangle_s. \qquad (7)$$

Spin-orbit resonances happen when spin precession is coherent with the disturbances experienced during synchro-betatron motions. The closed orbit spin tune satisfies the relation [9, 12]

$$\nu_0 = k + k_x Q_x + k_y Q_y + k_z Q_z, \qquad (8)$$

at spin-orbit resonances, where k, k_x, k_y, k_z are integers, and Q_x, Q_y, Q_z are tunes of synchro-betatron motions. The equilibrium polarization level will be lower near spin-orbit resonances due to the particularly strong spin diffusion.

POLARIZATION SIMULATIONS

The spin polarization simulations in the FCC-ee at Z energy have been explored using Bmad, to evaluate the effects of machine imperfections on the achievable polarization level. Bmad [16] is an accelerator simulation toolkit that includes modules for spin-orbit simulations. The Tao module [17] in Bmad is based on the SLIM formalism [8, 18] and allows simulations of linearized orbital and spin motions, while the Long-Term Tracking module [19] uses Monte-Carlo spin tracking which reveals the full impact of lattice perturbations on spin polarization.

The FCC-ee lattice of version 217 at Z energy without solenoid has been used in this study, with nominal energy being 45.6 GeV. The numbers of integration steps within different types of elements in spin-orbit tracking have been determined using convergence tests [20]. An effective model

as shown in Table 1 was created to generate small residual errors for different groups of elements in order to simulate the realistic orbits after lattice corrections. Misalignments of elements in three directions Δx, Δy, Δs, and angular misalignments around three axes $\Delta\theta$ (around $+y$ axis), $\Delta\phi$ (around $-x$ axis), $\Delta\psi$ (in $x - y$ plane) have been considered in the model. The values of misalignments are randomly generated, obeying truncated Gaussian distributions, truncated at $2.5\,\sigma$.

Linear Polarization Simulations

The influences of orbit distortions on equilibrium polarization in linear regime have been investigated via energy scans using the Tao module in Bmad. Figures 1 and 2 show the polarization levels at different energies using two error seeds generated from the effective model in Table 1. With the rms vertical orbit distortions of 43.7 µm and 148 µm at the nominal energy created by two seeds, equilibrium polarization levels of 91.56% and 83% can be achieved at 45.6 GeV respectively. A significant decrease of polarization can be observed when the machine operates near the first-order spin-orbit resonances $\nu_0 = k \pm Q_{x,y,z}$, where k is an integer and $Q_{x,y,z}$ represents synchro-betatron tunes.
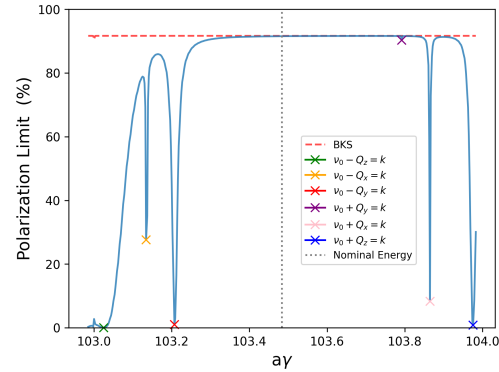

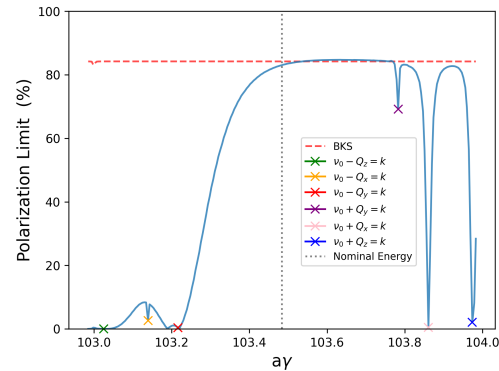Figure 1: Energy scan using error seeds with $(\Delta y)_{\mathrm{rms}} = 43.7$ µm

Figure 2: Energy scan using error seeds with $(\Delta y)_{\mathrm{rms}} = 148$ µm

Compared with asymptotic polarization P_{eq}, the ratio between polarization accumulation time and depolarization

65th ICFA Adv. Beam Dyn. Workshop High Luminosity Circular e⁺e⁻ Colliders
ISBN: 978-3-95450-236-3

eeFACT2022, Frascati, Italy

JACoW Publishing
ISSN: 2673-7027
doi:10.18429/JACoW-eeFACT2022-TUZAS0104

Table 1: An effective model for residual errors generation used in the spin-orbit simulations.

Type	$\sigma_{\Delta x}$ [μm]	$\sigma_{\Delta y}$ [μm]	$\sigma_{\Delta s}$ [μm]	$\sigma_{\Delta \psi}$ [μrad]	$\sigma_{\Delta \theta}$ [μrad]	$\sigma_{\Delta \phi}$ [μrad]
Arc quadrupole	0.1	0.1	0.1	2	2	2
Arc sextupole	0.1	0.1	0.1	2	2	2
Dipoles	0.1	0.1	0.1	2	0	0
IR quadrupole	0.1	0.1	0.1	2	2	2
IR sextupole	0.1	0.1	0.1	2	2	2

time τ_{bks}/τ_{dep} better reveals the depolarizing strength. It is related to the equilibrium polarization as

$$P_{eq} \simeq P_{bks} \frac{1}{1 + \tau_{bks}/\tau_{dep}}. \qquad (9)$$

Figures 3 and 4 show the depolarizing strengths at different energies using the same two error seeds as in Figure 1 and 2. It can be clearly seen that larger vertical orbit distortion results in a more significant depolarization effect at first-order spin-orbit resonances. The resonances are stronger near $a\gamma = 103$ compared to $a\gamma = 104$ due to periodic lattice structure and machine imperfections.

The energy scans of linear equilibrium spin polarization offer an illustration of the basic spin dynamics theory to first order, revealing the sensitivity of polarization curves to the orbits.
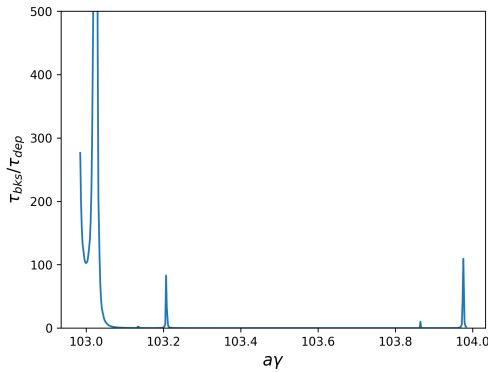

Figure 3: Depolarizing strength using error seeds with $(\Delta y)_{rms} = 43.7\,\mu m$

Nonlinear Spin Tracking Simulations

Linear spin simulations help to estimate the influence of first-order resonances. However, higher order spin resonances could be prominent at high energies and jeopardize the achievable polarization level. Nonlinear spin tracking simulations are therefore critical to evaluate the full impact of lattice imperfections on spins. The Long-Term Tracking module in Bmad has been used for Monte-Carlo spin tracking [19]. Starting from an initial level of P_0, the polarization build-up with time can be approximated as [9, 21]

$$P(t) = P_{dk} \left[1 - e^{-t/\tau_{dk}} \right] + P_0 e^{-t/\tau_{dk}} \qquad (10)$$
$$\simeq P_0 e^{-t/\tau_{dep}}.$$
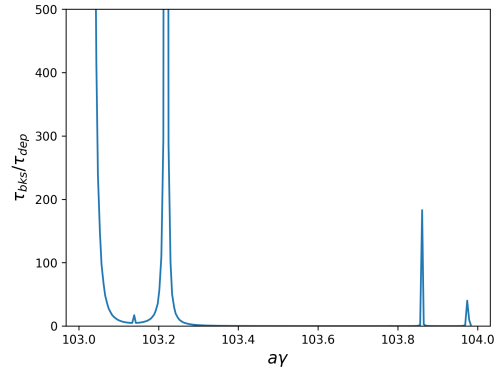

Figure 4: Depolarizing strength using error seeds with $(\Delta y)_{rms} = 148\,\mu m$

By tracking the polarization evolution of the initially polarized beam by turns, the depolarization rate τ_{dep} can be extracted by fitting the polarization build-up curve using Eq. (10). The equilibrium level can be estimated via Eq. (9), where P_{bks} and τ_{bks} can be computed in linear simulations.
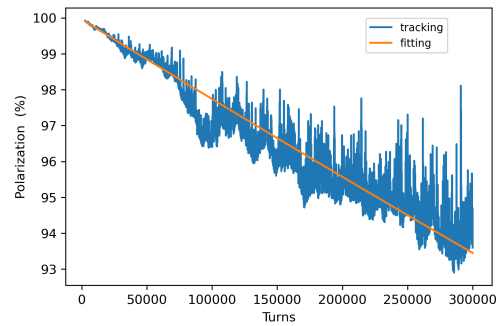

Figure 5: Polarization evolution of 10 electrons at $\nu_0 = k + Q_y - Q_z$

Figures 5 and 6 present two examples of polarization evolutions using 10 and 500 electrons respectively in nonlinear spin tracking simulations with PTC Bmad at one synchrotron sideband of the first-order vertical spin resonance $\nu_0 = k + Q_y - Q_z$. The equilibrium levels obtained from estimation are 0.15% and 0.099% respectively. Large fluctuations during evolution occur when using smaller amounts of particles as in Figure 5, resulting in R-squared value for data fitting evaluation being $R^2 \sim 0.89$, which indicates that the estimation accuracy is influenced in this case. The
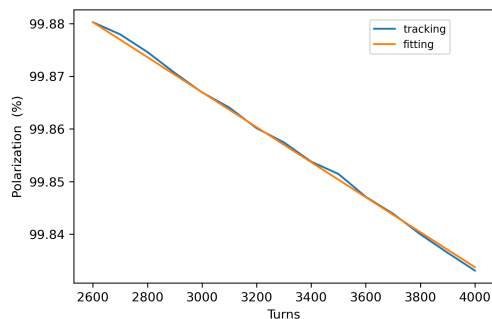
Figure 6: Polarization evolution of 500 electrons at $\nu_0 = k + Q_y - Q_z$

fitting precision is largely improved in the 500-electron case with $R^2 \sim 1$. Using a larger number of particles in nonlinear tracking enhances the estimation accuracy, while it also leads to a significant increase in the simulation time. Efforts will be made to overcome the challenges in simulation speed.
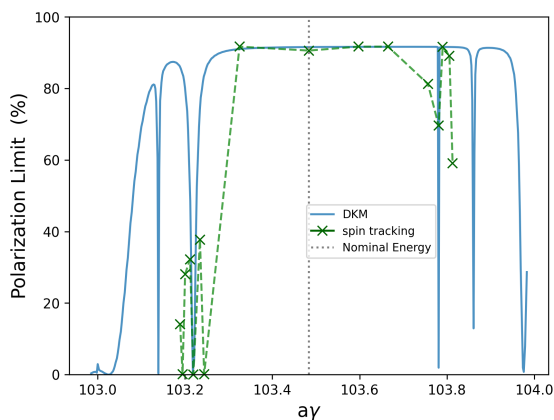

Figure 7: Polarization levels from linear and nonlinear spin simulations using the same error seed

A preliminary nonlinear spin tracking simulation has been conducted at several energies using 1000 particles tracked for 7000 turns via PTC Bmad. As shown in Figure 7, the nonlinear polarization is in good agreement with linear results. The first-order vertical resonances can be observed in both linear and nonlinear simulations, while higher order resonances such as two sidebands $\nu_0 = k + Q_y \pm Q_z$ can only be reflected in nonlinear spin tracking simulations. The equilibrium polarization near nominal energy remains sufficient for energy calibration.

CONCLUSION

High precision measurements are required in the FCC-ee to make the observation of new physics possible. Resonant depolarization is a promising method for the precise center-of-mass energy calibration in the FCC-ee at Z and W energies. A sufficient equilibrium polarization level should be guaranteed for this energy calibration method.

The early-stage explorations of the spin simulations in the FCC-ee using Bmad have been presented. The linear spin simulations reveal the depolarization effects near first-order spin-orbit resonances, while nonlinear spin trackings reflect all impacts of lattice perturbations. The sensitivity of spin polarization to lattice imperfections has been verified, which highlights the demand for a good closed orbit control. This work offers a promising outlook for the spin polarization studies in the FCC-ee.

REFERENCES

[1] A. Abada *et al.*, "FCC Physics Opportunities: Future Circular Collider Conceptual Design Report Volume 1," *European Physical Journal C*, vol. 79, no. 6, p. 474, 2019.

[2] A. Abada *et al.*, "FCC-ee: The Lepton Collider: Future Circular Collider Conceptual Design Report Volume 2," *European Physical Journal: Special Topics*, vol. 228, no. 2, pp. 261–623, 2019.

[3] A. Blondel, "PED Overview: Centre-of-mass energy calibration." https://indico.cern.ch/event/1064327/contributions/4893236/attachments/2452727/4203106/EPOL%202022-05-30.pdf.

[4] R. Assmann *et al.*, "The energy calibration of LEP in the 1993 scan," *Zeitschrift für Physik C Particles and Fields*, vol. 66, no. 4, pp. 567–582, 1995.

[5] A. Blondel *et al.*, "Polarization and Centre-of-mass Energy Calibration at FCC-ee," *arXiv preprint arXiv:1909.12245*, 2019.

[6] L. H. Thomas, "The kinematics of an electron with an axis," *The London, Edinburgh, and Dublin Philosophical Magazine and Journal of Science*, vol. 3, no. 13, pp. 1–22, 1927.

[7] V. Bargmann, L. Michel, and V. Telegdi, "Precession of the polarization of particles moving in a homogeneous electromagnetic field," *Physical Review Letters*, vol. 2, no. 10, p. 435, 1959.

[8] A. W. Chao, *Special Topics in Accelerator Physics*. World Scientific, 2022.

[9] A. W. Chao *et al.*, *Handbook of accelerator physics and engineering*. World scientific, 2013.

[10] D. P. Barber, "An Introduction to Spin Polarisation in Accelerators and Storage Rings." https://www.desy.de/~mpybar/CI-lectures-2014.pdf.

[11] A. Sokolov and M. Ternov, "On polarization and spin effects in the theory of synchrotron radiation," in *Sov. Phys.-Dokl.*, vol. 8, pp. 1203–1205, 1964.

[12] D. P. Barber, "Spin Dynamics and Simulation of Spin Motion in Storage Rings," in *AIP Conference Proceedings*, vol. 1008, pp. 82–90, American Institute of Physics, 2008.

[13] V. Baier, V. Katkov, and V. Strakhovenko, "Kinetics of Radiative Polarization," *Sov. Phys. JETP*, vol. 31, p. 908, 1970.

[14] Y. S. Derbenev and A. Kondratenko, "Polarization kinetics of particles in storage rings," *Sov. Phys. JETP*, vol. 37, no. 6, pp. 968–973, 1973.

[15] S. R. Mane, "Derivation of the equilibrium degree of polarization in high-energy electron storage rings," *Physical Review Letters*, vol. 57, no. 1, p. 78, 1986.

[16] D. Sagan, "Bmad, a subroutine library for relativistic charged-particle dynamics." `https://www.classe.cornell.edu/bmad`.

[17] D. Sagan, "The Tao Manual." `https://www.classe.cornell.edu/bmad/tao.html`.

[18] A. W. Chao, "Evaluation of Radiative Spin Polarization in an Electron Storage Ring," *Nuclear Instruments and Methods*, vol. 180, no. 1, pp. 29–36, 1981.

[19] D. Sagan, "Long Term Tracking Program." `https://www.classe.cornell.edu/bmad/other_manuals.html`, 2021.

[20] Y. Wu, "First Exploration of Spin Dynamics Simulations in FCC-ee for Depolarization Based Energy Calibration." presented at FCC Week May-June 2022, Sorbonne Université, Paris, France, `https://indico.cern.ch/event/923801/contributions/4893334/`.

[21] E. Gianfelice-Wendt, "The polarization code challenge." presented at FCC Week Nov. 2020, `https://indico.cern.ch/event/923801/contributions/4044076/`.